Microtensile strain on the corrosion performance of diamond-like carbon coating

Seung-Hwan Lee,[1] Jung-Gu Kim,[1] Heon-Woong Choi,[2] Kwang-Ryeol Lee[2]
[1]*Department of Advanced Materials Engineering, Sungkyunkwan University, 300 Chunchun-Dong, Jangan-Gu, Suwon 440-746, Korea*
[2]*Future Technology Research Division, Korea Institute of Science and Technology, P.O. Box 131, Cheongryang, Sungbuk-Gu, Seoul 130-650, Korea*

Received 10 March 2007; revised 13 June 2007; accepted 26 June 2007
Published online 26 September 2007 in Wiley InterScience (www.interscience.wiley.com). DOI: 10.1002/jbm.a.31597

Abstract: Hydrogenated diamond-like carbon films (a-C:H DLC) were deposited on STS 304 substrates for the fabrication of vascular stents by means of the r.f. plasma-assisted chemical vapor deposition technique. This study provides reliable and quantitative data for the assessment of the effect of strain on the corrosion performance of DLC-coated systems in the simulated body fluid obtained through electrochemical techniques (potentiodynamic polarization test and electrochemical impedance spectroscopy) and surface analysis (scanning electron microscopy). The electrolyte used in this test was 0.89% NaCl solution at pH 7.4 and 37°C. It was found that the corrosion resistance of the plastically deformed DLC coating was insufficient for use as a protective film in a corrosive body environment. This is due to the increase in the delamination area and degradation of the substrate's corrosion properties with increasing tensile deformation. © 2007 Wiley Periodicals, Inc. J Biomed Mater Res 85A: 808–814, 2008

Key words: diamond-like carbon; stent; microtensile test; electrochemical impedance spectroscopy; potentiodynamic polarization test

INTRODUCTION

Using protective films to coating implants, in order to reduce their level of corrosion and wear, may extend their lifetime to the benefit of the patients. Diamond-like carbon (DLC), which is characterized by chemical inertness, corrosion, and wear resistance, appears to be an ideal material for such purposes.[1] Because of its bio- and hemocompatible nature,[2–5] there is a growing interest in the application of DLC to orthopedic and blood contacting implants.[6] Today, there are two main areas of application of DLC in biological applications, namely in blood contacting implants such as heart valves and stents, and in load bearing joints to reduce the level of wear. The load-bearing properties of the implants are mainly controlled by their bulk properties, whereas the interaction with the surrounding tissue is governed by the implant surface.[7] Neither natural diamond nor DLC coatings cause tissue reactions, and the corrosion of implants can be decreased significantly by using such a coating.[8] However, the high hardness, intrinsic stresses, and poor adhesion of these materials limit their area of application. These negative effects are especially pronounced when the coatings are applied to relatively soft substrates such as steels. Such problems have been reduced using a multilayer design, in which metal and ceramic layers are used to increase the strength of adhesion, relax the compressive stress of the DLC film, and increase the load support capability.[9,10] One or more interim layers are introduced to improve the adhesion of the DLC to the metallic substrate. Moreover, the adhesion of a DLC film with an intermediate layer of a-SiC_x or TiC was found to be significantly improved.[4,11–13] However, a report on DLC coatings in total hip arthroplasty (THA) showed delamination and brittling under *in vivo* conditions, and it was observed that the spallation of the DLC coating during the experiment simulated the expansion of the vascular stent. The DLC coating on stainless steel used to prevent the elution of Ni and Cr should survive the plastic deformation of the substrate.[14,15] In this paper, we focused on evaluating the

Correspondence to: J.-G. Kim; e-mail: kimjg@skku.ac.kr
Contract grant sponsor: Center for Nanostructured Materials Technology (21st Century Frontier R&D Programs of the Ministry of Science and Technology, Korea); contract grant number: 06K1501-01610

variation of the corrosion performance of the DLC coating with strain (maximum 4%) during the expansion of the vascular stent through electrochemical techniques.

MATERIALS AND METHODS

A 304 stainless steel with a thickness of 0.2 mm was used as the substrate material, and was electrochemically polished to obtain an rms surface roughness of less than 0.1 μm. Before deposition, the substrates were precleaned using an argon plasma for 60 min at a bias voltage of −900 V. A Si interlayer with a thickness of ~ 98 nm was deposited onto the substrate prior to the DLC coating, in order to improve the adhesion between the coating and substrate. The DLC films were deposited by the radio frequency plasma-assisted chemical vapor deposition (r.f. PACVD) method using benzene as the precursor gas. The residual compressive stress and hardness of the DLC films in this work were 0.9 and 10 GPa, respectively. The detailed deposition conditions are given in Table I.

Electrochemical techniques were used to evaluate the influence of the microtensile strain on the corrosion performance. The potentiodynamic polarization test was performed with an EG&G Princeton Applied Research model 273A potentiostat. The potentiodynamic polarization test was carried out in a 0.89% NaCl solution at pH 7.4 and 37°C, which was thoroughly deaerated by bubbling high purity nitrogen gas for 0.5 h prior to the immersion of the specimen and continuously purged during the test. The exposed specimen area was 0.25 cm^2. A saturated calomel electrode and pure graphite were used for the reference and counter electrodes, respectively. Prior to the potentiodynamic polarization test, the specimens were kept in the solution for 3 h to obtain a stabilized open-circuit potential. The potential of the electrode was swept at a rate of 0.166 mV/s from the bottom potential of −250 mV versus E_{corr} to the top potential of 1600 mV. The porosity and protective efficiency of the DLC coating were estimated using the potentiodynamic polarization, and the delamination area was estimated using the electrochemical impedance spectroscopy (EIS) test. Matthes et al.[16] established an empirical equation to estimate the porosity of coatings:

$$P = \frac{R_{pm(substrate)}}{R_{p(coating-substrate)}} \times 10^{-|\Delta E_{corr}\beta_a|} \quad (1)$$

where P is the total coating porosity, R_{pm} the polarization resistance of the substrate, and R_p the measured polarization resistance of the coated system. ΔE_{corr} is the potential difference between the corrosion potentials of the coated steel and the bare substrate, and β_a the anodic Tafel slope for the substrate. Also, the protective efficiency of the coating was determined from the polarization curve by means of Eq. (2):

$$P_i = 100\ (1 - i_{corr}/i^o_{corr}) \quad (2)$$

where i_{corr} and i^o_{corr} indicate the corrosion current densities in the presence and absence of the coating, respectively.[17]

EIS is a nondestructive testing method frequently used for assessing the protective performance of coatings. A Zahner IM6e system using a commercial software (THALES) program for AC measurement was used to obtain the EIS data. The impedance measurements were performed by applying a sinusoidal wave with an amplitude of 10 mV to the working electrode, at frequencies ranging from 10 kHz to 10 mHz. The impedance diagrams were interpreted on the basis of the equivalent circuit using the THALES fitting program. The delamination area of the coatings exposed to the electrolyte was determined using EIS. Thus, the extent of the delamination area could be determined from the experimental values of the pore resistance obtained from the impedance diagrams on the basis of the equivalent circuit. The pore resistance of the coating is related to the delamination area, that is, the pore resistance decreases as the delaminated area increases. Therefore, the delamination area was calculated by means of the following equations.

$$A_d = R^o_{pore}/R_{pore} \quad (3)$$

$$R^o_{pore} = \rho d\ (\text{ohm cm}^2) \quad (4)$$

where R^o_{pore} is the characteristic value for the corrosion reaction at the solution–coating interface, d is the coating thickness, and ρ is the coating resistivity.

Scanning electron microscopy (SEM) was used to examine the delamination and spallation of the coatings after the EIS test, and 500× and 2000× SEM images were

TABLE I
Main Deposition Conditions

Deposition method	r.f. PACVD (13.56 MHz)
Base pressure	2.0×10^{-5} Pa
Interlayer	Silicon interlayer
Precleaning time	60 min (Ar sputtering)
DLC precursor gas	C_6H_6
Deposition pressure	2.0×10^{-2} Pa
Bias voltage (deposion/precleaning)	−400 V/−900 V
Si interlayer thickness	98 nm
Film thickness	1 μm

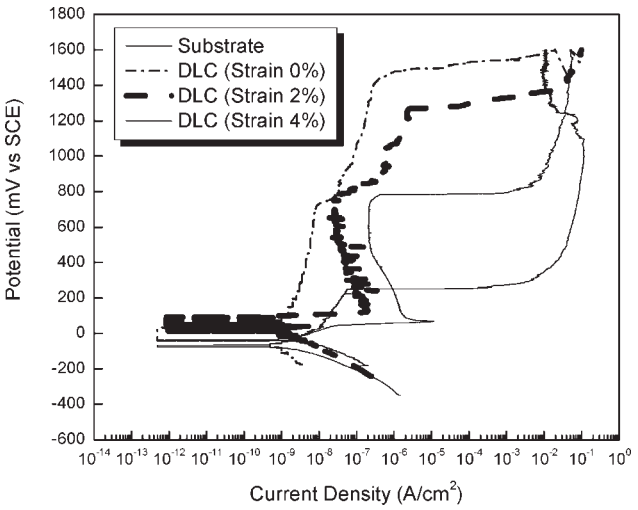

Figure 1. Potentiodynamic polarization curves in deaerated 0.89% NaCl solution at 37°C (pH 7.4).

TABLE II
Results of Potentiodynamic Tests

	E_{corr} (mV)	i_{corr} (nA/cm^2)	β_a (V/decade)	β_c (V/decade)	R_p (10^3 Ω cm^2)	Protective Efficiency (%)	Porosity
Sub	−33.9	6.557	0.2981	0.0693	3726.2217	–	–
0%	−32.55	0.312	0.2284	0.1425	122441.5576	95.25	0.0301
2%	−29.86	1.126	0.4851	0.1137	35566.7122	82.83	0.1015
4%	−69.32	4.720	0.1000	0.1041	4698.2691	28.02	0.6033

obtained for this purpose. A SE detector was used and the acceleration voltage was 15 keV.

RESULTS AND DISSCUSION

The protective ability of the coating was investigated using the potentiodynamic polarization test. The polarization curves of the DLC coatings and substrate in the simulated body fluid are shown in Figure 1. The measured potentiodynamic polarization test results, such as the corrosion potential (E_{corr}), corrosion current density (i_{corr}), porosity (P), and protective efficiency (P_i) are shown in Table II. The corrosion current densities were 6.557 nA/cm^2 for the substrate, 0.312 nA/cm^2 for the 0%-strained coated system, 1.126 nA/cm^2 for the 2%-strained coated system, and 4.720 nA/cm^2 for the 4%-strained coated system. The corrosion current densities for the coated systems were lower than that for the substrate. This means that the coating with fewer pores makes the substrate more passive than the coating with a larger number of pores. In this solution, substrate and DLC coatings exhibited passive behavior. However, as the strain increased, DLC coatings suffered active-to-passive transitions and the pitting potential also decreased, which were indicative of active dissolution or incomplete passivity. This causes a high local current density and induces high metal dissolution at anode. Another possible mechanism may involve a periodic galvanic interaction between DLC coating and the uncovered stainless steel. As a result of an electrochemical potential difference between the substrate and DLC film, a small electrical current is generated between the anodic metal and the cathodic film. The relatively small area of the substrate metal surface compared to the large surface area of DLC film results in an unfavorable anode-to-cathode ratio. These pores can weaken the interfacial material and provide a path for metallic ions and corrosive agents. The lower the calculated porosity, the lower the corrosion current density. The protective efficiency of the coating decreases as the tensile deformation proceeds, and is appreciable after plastic deformation. The 0%-strained coating shows the best protective efficiency of 95.25%, and this result is closely related to the po-

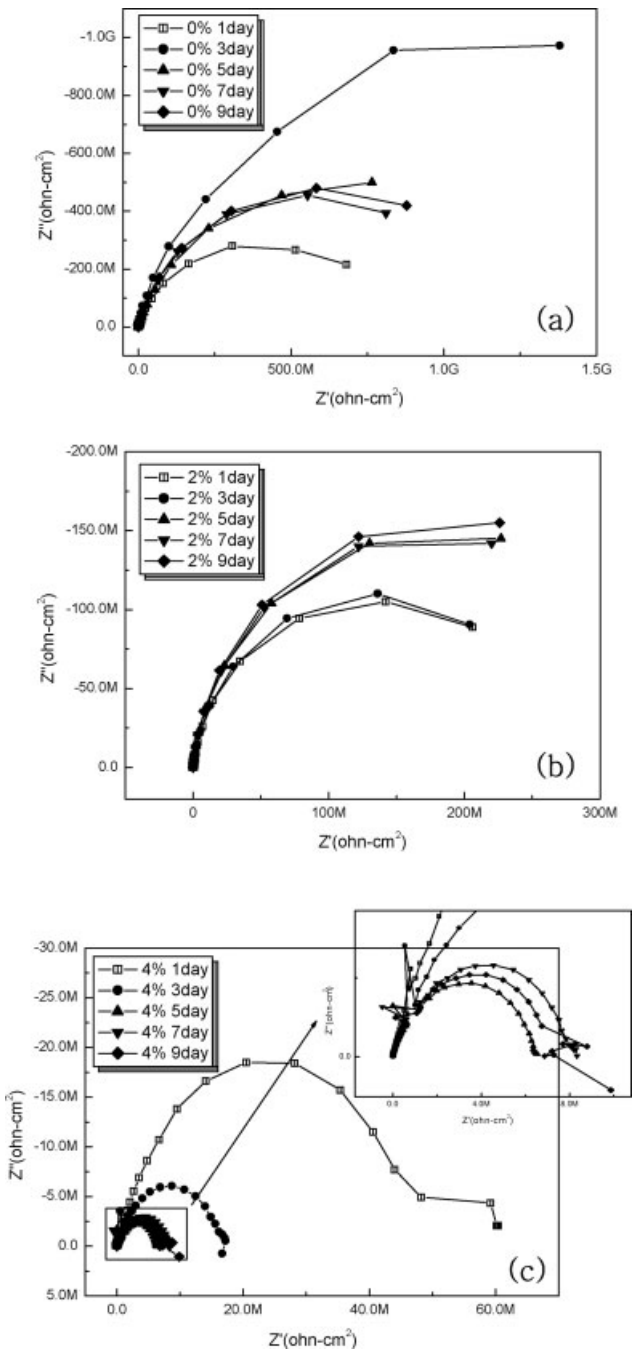

Figure 2. Nyquist plots for (a) 0%, (b) 2%, and (c) 4%-strained specimens.

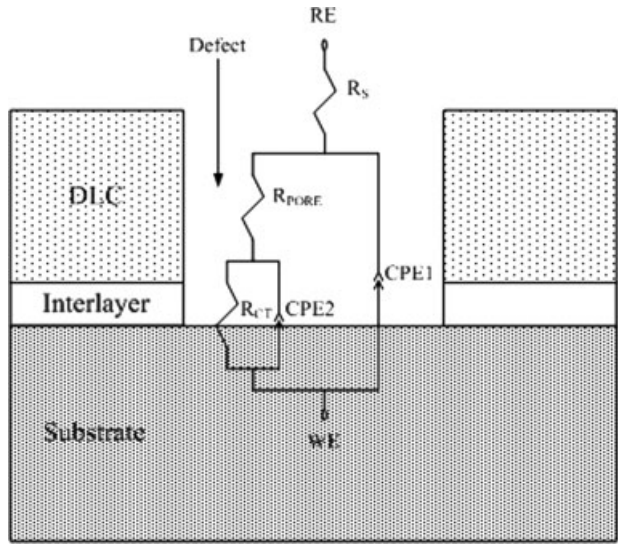

Figure 3. Equivalent circuit for the DLC film systems. (WE: working electrode, RE: reference electrode).

rosity. The protective efficiency increases as the porosity decreases and, consequently, the best corrosion resistance and durability are obtained for the coating with fewer pores and lower strain.

Nyquist plots of DLC-coated specimens with different strain are shown in Figure 2. The interpretation of the EIS measurements is usually done by fitting the impedance data to an equivalent circuit, which is representative of the physical processes taking place in the system under investigation. The electrochemical response during the EIS measurements for the DLC coatings was best simulated with the equivalent circuit, as shown in Figure 3. The results of EIS measurements were given in Table 3. The equivalent circuit consists of the following elements: R_s is the solution resistance of the test electrolyte between the working electrode and the reference electrode, and C_{coat} is the coating capacitance generated by the dielectric properties of the coating. C_{coat} corresponds to the dielectric strength of the coating and the water absorption by the coating. Higher values indicate higher dielectric strength or higher water content. R_{pore} is the electrical resistance resulting from the formation of ionic conduction paths through the pores in the coating. Higher values indicate higher resistance to penetration of corrosive species. C_{dl} is the capacitance generated by the electric double layer at the water/substrate interface. An appreciable C_{dl} value indicates that water is present at the substrate. Higher values of C_{dl} indicate a greater wetted area of substrate. R_{ct} is the charge-transfer resistance of the substrate to corrosion. Higher values indicate lower rates of corrosion. Constant phase elements (CPEs) are used in the data fitting, to allow for depressed semicircles. The capacitances are replaced with CPEs in order to improve the quality of the fit. The CPEs are, in fact, a general expression for many circuit elements. In this paper, C_{coat} and C_{dl} are replaced with CPE1 and CPE2, respectively.

The variations of the capacitance are indicated in Figure 4(a,b). In the case of 4% strain, it is shown that the capacitance increases significantly with increasing immersion time, whereas the 0% and 2%-strained coatings show only a slight increase or a small variation. This is because the coating with the 4% plastic deformation has more pores and allows more water to be adsorbed by the substrate. As shown in Figure 4(c), the pore resistance (R_{pore}) of the coatings decreases gradually with increasing immersion time. The coating may swell, and the number and size of the pores increase. The decrease in the pore resistance of the coating corresponds to the occurrence of water saturation, as depicted by the increase of the

TABLE III
Results of Electrochemical Impedance Spectroscopy Measurements

Exposure Time			CPE1			CPE2		
		R_s (Ω cm^2)	C_{coat} (10^{-9} F/cm^2)	n (0–1)	R_{pore} (10^{-3} Ω cm^2)	C_{dl} (10^{-9} F/cm^2)	n (0–1)	R_{ct} (10^3 Ω cm^2)
24 h	Strain 0%	202.6	2.355	0.9094	6.063	2.171	1	3621
	Strain 2%	5.32	29.18	0.8774	2.071	19.39	1	221.3
	Strain 4%	4.383	394.7	1	1.355	472.9	0.7311	52.57
72 h	Strain 0%	89.79	1.871	0.9103	2.047	4.195	0.9188	3166
	Strain 2%	13.01	29.59	0.8822	1.326	59.52	0.9304	146.1
	Strain 4%	1.927	152.5	0.6917	0.2207	415.5	1	17.67
120 h	Strain 0%	100.8	2.04	0.8834	2.613	7.85	0.2753	1008
	Strain 2%	10.06	36.07	0.8367	1.461	100.8	0.8321	118.3
	Strain 4%	2.825	181.3	1	0.1842	575.9	0.666	8.505
168 h	Strain 0%	52.63	2.151	0.8842	2.657	6.019	0.194	772
	Strain 2%	33.12	47.85	0.8614	1.313	120.7	0.7967	109.6
	Strain 4%	1.037	445.3	0.9074	0.1961	608.9	0.719	6.035
216 h	Strain 0%	1.609	2.33	0.8813	2.73	7.44	0.937	726.1
	Strain 2%	10.03	52.29	0.8238	0.8094	193.9	0.799	100.8
	Strain 4%	9.997	654.6	0.9074	0.1047	778	0.712	5.559

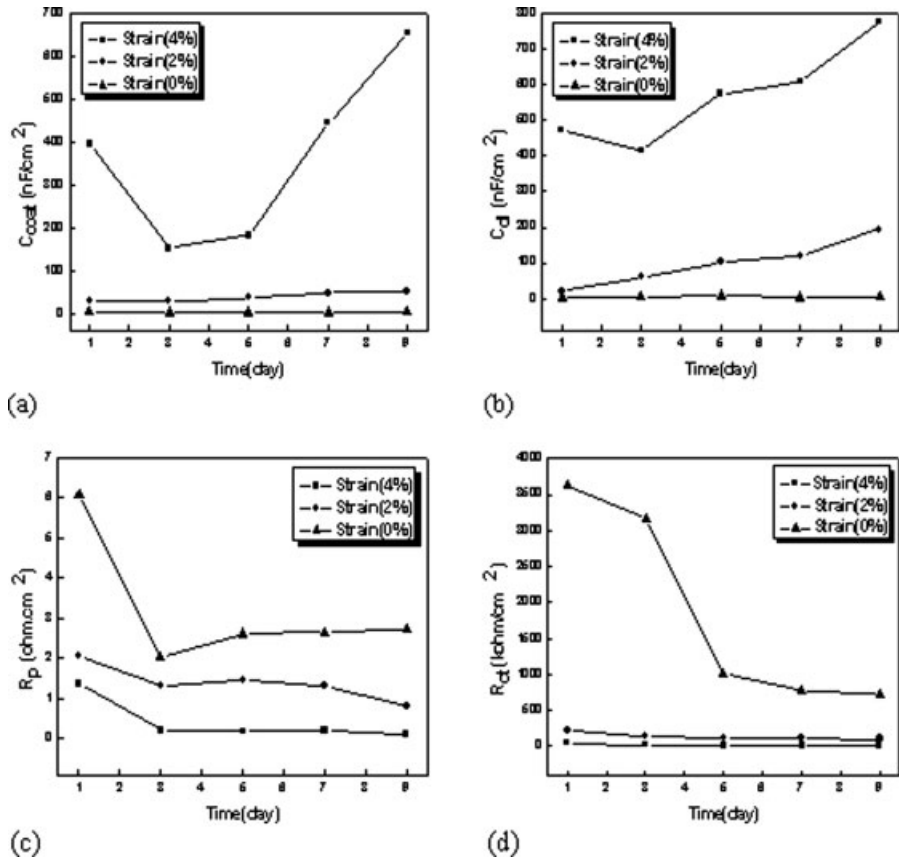

Figure 4. (a) Coating capacitance, (b) double-layer capacitance, (c) pore resistance, (d) charge-transfer resistance.

coating capacitance. Also, the pore resistance of the coating decreases as more ions and water reach the coating surface, causing an increased electrochemical reaction. According to Figure 4(d), the charge transfer resistance (R_{ct}) decreased with increasing immersion time. This means that water and ions would have gradually migrated to the substrate surface. The charge-transfer resistance of the less strained coating is higher than that of the more strained one. The plastic deformation of the specimen resulted in the film rupture process, which is consistent with the reduction of the resistance.

Also, the results obtained from the EIS measurements are usually used to monitor the change of the delamination area (A_d). Figure 5 shows the delamination areas of the three kinds of DLC coatings. The delamination area of the coating with 4% strain increases significantly with increasing immersion time, as shown in Figure 5. On the other hand, the delamination areas of the coatings with 0 and 2% strain show only a slight increase or become stabilized with increasing immersion time. The delamination area is affected by the penetration of water through the porous coating, because water saturation in the coating/substrate interface leads to delamination and blistering. Consequently, the delamination area is much lower in the coating with lower strain than in that with higher strain. It is clear that the delamination area is closely related to the penetration of water through the pores and defects. Structural defects, such as pinholes, pores, and cracks, act as channels for the corrosion of the substrate. The porosity of the coating is the main cause of coating delamination.

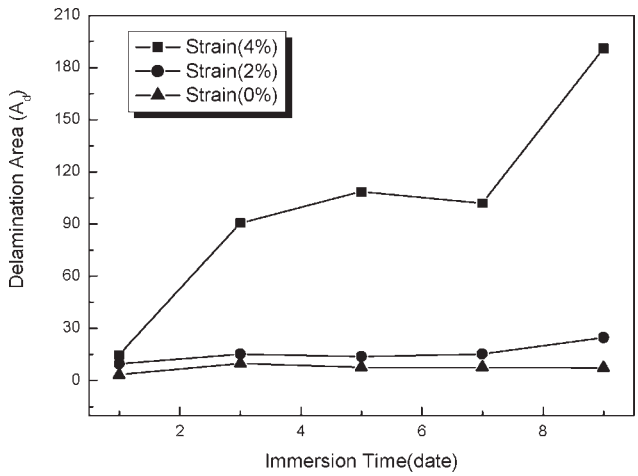

Figure 5. Delamination area as a function of immersion time.

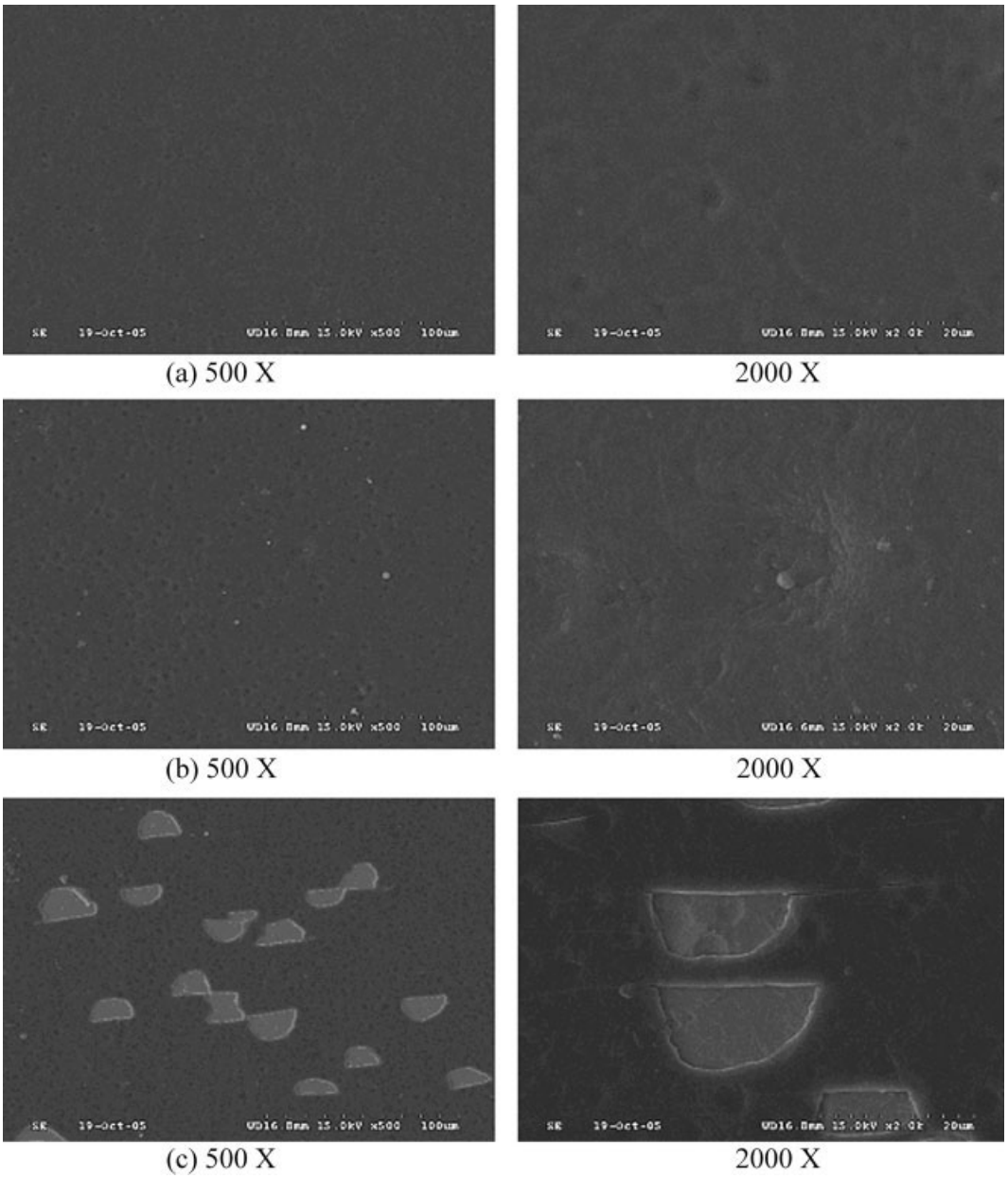

Figure 6. SEM microstructures of the specimen surface after imposing tensile strains of (a) 0%, (b) 2%, and (c) 4%-strained.

After the completion of the EIS test, the morphology and corrosion features of the DLC-coated systems with 0, 2, and 4% micro-tensile strain were inspected by SEM and the resulting micrographs are shown in Figure 6. Choi et al.[15] show that the yield point of the specimen is between 3 and 4% strain in the force–strain curve. When the stainless steel substrate was elastically deformed, there were no appreciable defects in the film. However, after the stainless steel substrate was plastically deformed (4%-strained), crack propagation occurred along the slip directions. This means that the tensile strain of the substrate affects the integrity of coating; thus, the plastic deformation is closely related with the protective ability of coating. Since the elution of Ni and Cr through spallation has a deleterious effect on the human body,[15] the coating system with higher stress corrosion resistance is more adequate for protective films in the body environments.

CONCLUSIONS

Using electrochemical techniques and surface analysis, the corrosion behavior of DLC coatings on 304 stainless steel substrates subjected to different levels of tensile strain was investigated.

1. The DLC coatings with lower strain showed a lower corrosion current density and porosity than the plastically deformed coating, indicating that the former had better corrosion resistance.
2. Decreasing the level of stain reduced the delamination area in the DLC coatings. Also, the charge-transfer resistance values of the coated system increased as the stain decreased.
3. When the stainless steel substrate was plastically deformed, an increase in the delamination area and spallation behavior of the coating was observed in the EIS and SEM analyses, which means that plastic deformation decreases the protective ability of the DLC coating.
4. Consequently, the corrosion performance of DLC coatings decreased as the strain increased, which was caused by galvanic coupling between DLC coating and the uncovered stainless steel through the film rupture.

References

1. Grill A. Diamond-like carbon coatings as biocompatible materials An overview. Diamond Relat Mater 2000;12:166–170.
2. Allen M, Law F, Rushton N. The effects of diamond-like carbon coatings on macrophages, fibroblasts and osteoblast-like cells in vitro. Clin Mater 1994;17:1–10.
3. Butter R, Allen M, Chandra L, Lettington AH, Rushton N. In vitro studies of DLC coatings with silicon intermediate layer. Diamond Relat Mater 1995;4:857–861.
4. Stuber M, Ulrich S, Leiste H, Kratzsch A, Hollek H. Graded layer design for stress-reduced and strongly adherent superhard amorphous carbon films. Surf Coat Technol 1999;116–119:591–598.
5. Jones MJ, McColl IR, Grant DM, Parker KG, Parker TL. Protein adsorption and platelet attachment and activation, on TiN, TiC, and DLC coatings on titanium for cardiovascular applications. J Biomed Mater Res 2000;52:413–421.
6. Hauert R, Muller U. An overview on tailored tribological and biological behavior of diamond-like carbon. Diamond Relat Mater 2003;12:171–177.
7. Hauert R. A review of modified DLC coatings for biological applications. Diamond Relat Mater 2003;12:583–589.
8. Morshed MM, McNamara BP, Cameron DC, Hashmi MSJ. Effect of surface treatment on the adhesion of DLC film on 316L stainless steel. Surf Coat Technol 2003;163–164:541–545.
9. Voevodin AA, Walck SD, Zabinski JS. Architecture of multilayer nano-composite coatings with super-hard diamond-like carbon layers for wear protection at high contact loads. Wear 1997:203–204:516–527.
10. Chen CC, Hong FCN. Interfacial studies for improving the adhesion of diamond-like carbon films on steel. Appl Surf Sci 2005;243:296–303.
11. Yin GF, Luo JM, Zheng CQ, Tong HH, Huo YF, Mu LL. Preparation of DLC gradient biomaterials by means of plasma source ion implant-ion beam enhanced deposition. Thin Solid Films 1999;345:67–70.
12. Liu Y, Meletis EI. Tribological behavior of DLC coatings with functionally gradient Interfaces. Surf Coat Technol 2002;153:178–183.
13. Lung BH, Chiang MJ, Hon MH. Effect of gradient a-SiC*x* interlayer on adhesion of DLC films. Mater Chem Phys 2001;72:163–166.
14. Taeger G, Pldleska LE, Schmidt B, Ziegler M, Nast-Kolb D. Comparison of diamond-like-carbon and alumina-oxide articulating with polyethylene in total hip arthroplasty. Mat.-wiss. u. Werkstoffteck 2003;34:1094–1100.
15. Choi HW, Lee KR, Wang R, Oh KH. Fracture behavior of diamond-like carbon films on stainless steel under a micro-tensile test condition. Diamond Relat Mater 2006;15:38–43.
16. Matthes B, Brozeit E, Aromaa J, Ronkainen H, Hannula SP, Leyland A, Matthews A. Corrosion porfomance of some titanium-based hard coatings. Surf Coat Technol 1991;49:489–495.
17. Yu YJ, Kim JG, Cho SH, Boo JH. Plasma-polymerized toluene films for corrosion inhibition in microelectronic devices. Surf Coat Technol 2003;162:161–166.